

Exploring Pyrazole and Diazepine Derivatives: Advances in Molecular Docking, Synthesis, and Biological Activities

Dina Saleem¹ , Zinah Hussein Ali¹, Noor Waleed Ibrahim², Abbas K. Abbas³ ,
Toqa Monther Abd-Almonaem¹ , Mastafa H. Al-Musawi⁴ , Mahmoud Gharbavi^{5*} 

1. College of Pharmacy, AL-Mustansiriyah University, Baghdad, Iraq
2. Department of Pharmaceutical Chemistry, College of Pharmacy, Mustansiriyyah University, Baghdad, Iraq
3. Muthanna Agriculture Directorate, Ministry of Agriculture, Al-Muthanna, Iraq
4. Department of Biology, College of Science, Mustansiriyyah University, Baghdad, Iraq
5. Nanotechnology Research Center, Medical Basic Sciences Research Institute, Ahvaz Jundishapur University of Medical Sciences, Ahvaz, Iran



Article Info

doi [10.30699/jambr.33.161.358](https://doi.org/10.30699/jambr.33.161.358)

Received: 2025/09/20;

Accepted: 2025/12/07;

Published Online: 12 Dec 2025;

Use your device to scan and read the article online



*Corresponding author:

Mahmoud Gharbavi,

Nanotechnology Research Center,
Medical Basic Sciences Research
Institute, Ahvaz Jundishapur
University of Medical Sciences, Ahvaz,
Iran

Email: gharbavi1981@gmail.com

ABSTRACT

Background & Objective: This study focuses on the synthesis and evaluation of a series of new pyrazole and diazepine derivatives, which are significant heterocyclic compounds known for their biological and pharmacological potential. The primary objectives were to characterize the synthesized compounds, investigate their inhibitory potential against glucosamine-6-phosphate synthase via molecular docking, and evaluate their antibacterial and anticancer activities.

Materials & Methods: The derivatives were prepared using conventional organic methods from chalcone intermediates derived from 4-aminoacetophenone, which reacted with various substituted anilines. Structural confirmation was achieved using FT-IR and ¹HNMR spectroscopy. Molecular docking studies were performed to assess the binding affinities and interactions of the compounds with glucosamine-6-phosphate synthase. Biological evaluation included testing antibacterial activity against *E. coli* and *S. aureus* and assessing cytotoxicity against the MCF-7 breast cancer cell line.

Results: Molecular docking revealed that both the pyrazole and diazepine derivatives exhibited favorable binding affinities for glucosamine-6-phosphate synthase by forming multiple stabilizing interactions within the enzyme's active site, suggesting a promising potential as enzyme inhibitors. Biological evaluation showed that some derivatives had considerable antibacterial activity, with compound 5 being especially effective against *E. coli* and *S. aureus*; its efficacy increased with concentration. Additionally, derivative 5 demonstrated notable cytotoxicity against the MCF-7 breast cancer cell line, reducing cell viability in a clear dose-dependent manner.

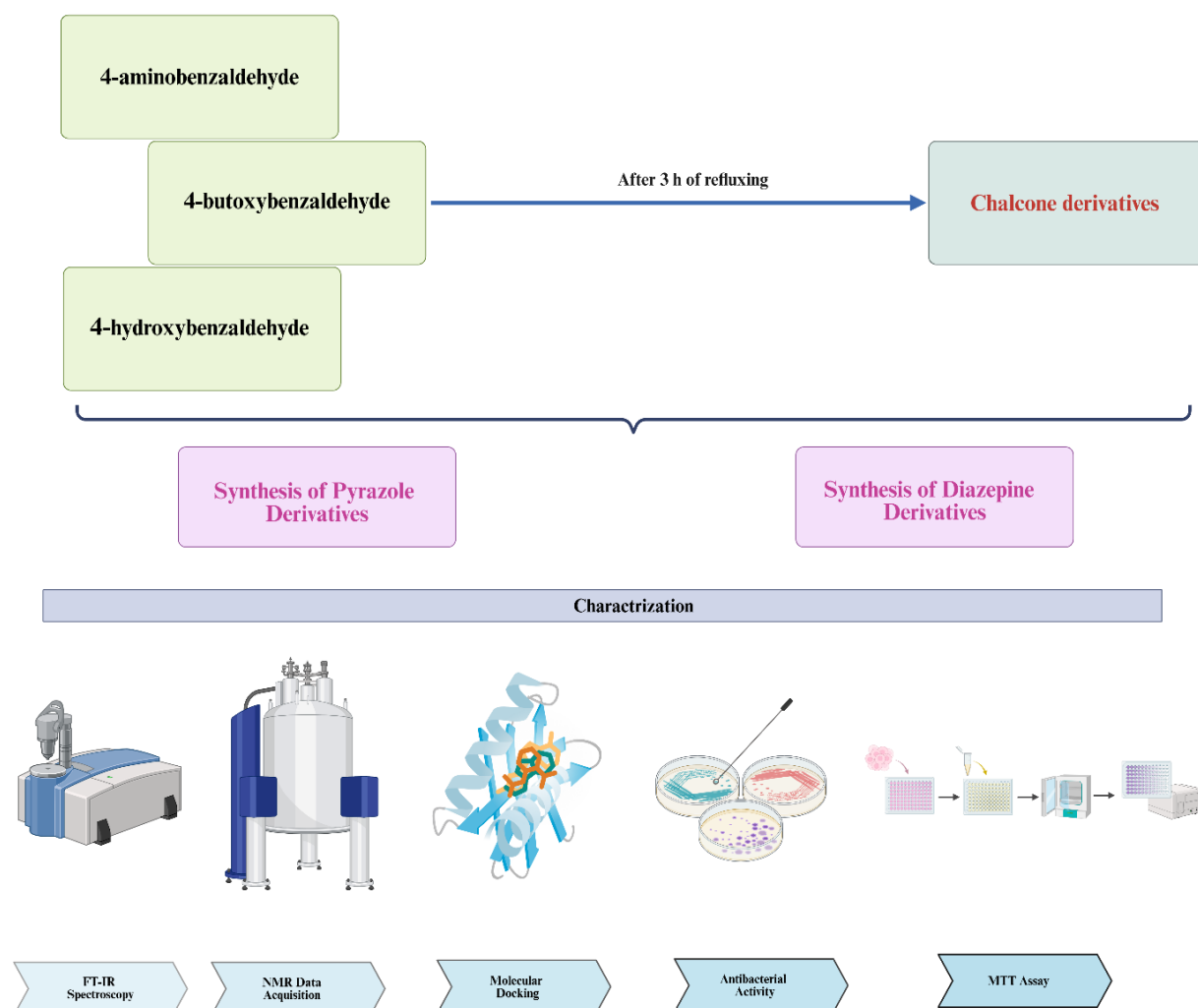
Conclusion: The comprehensive study confirmed that the new pyrazole and diazepine derivatives, characterized through synthesis and spectroscopy, are promising antibacterial and anticancer leads due to favorable molecular docking profiles and demonstrated structure-activity relationships, warranting future optimization.

Keywords: Antibacterial Activity, Anticancer Agents, Chalcone Synthesis, Drug Discovery, Molecular Docking



Copyright © 2025, This is an original open-access article distributed under the terms of the [Creative Commons Attribution-noncommercial 4.0 International License](https://creativecommons.org/licenses/by-nc/4.0/) which permits copy and redistribution of the material just in noncommercial usages with proper citation.

Graphical Abstract



(Prepared by Authors, 2025)

1. Introduction

The importance of pyrazole and diazepine derivatives contrasts with their heterocyclic nature in possessing a plethora of biological and pharmacological potential. Pyrazoles display a five-membered ring containing two adjacent nitrogen atoms, while diazepines exhibit seven-membered ring harbouring two nitrogen atoms. Both have been extensively investigated in medical chemistry due to their antibacterial and anticancer activities (1).

Besides the threat of antibiotic resistance worldwide and the subsequent demand for new chemotherapeutic agents, a significant reason for this research is given by heterocyclic compounds like pyrazoles and diazepines, which are abundantly found in nature and pharmaceutical products and are extremely relevant for drug discovery (2). Their unique framework allows interaction with a multitude of biological targets, thus making them suitable for novel treatments that would be developed against resistant bacteria and cancer (3).

Significant work has been performed on this subject, but important gaps still exist in the understanding of structure-activity relationships, optimum synthesis, and the relevant biological evaluation of such derivatives (4). In most cases of previous studies, either synthesis or biological activity evaluation was carried out in isolation; very few could integrate molecular docking, synthesis, and biological assessment under one roof. This article fills the gaps identified above in considering all the approaches investigated, leading to a comprehensive understanding of these compounds' prospects (5).

Glucosamine-6-phosphate synthase (GP6 synthase) is a crucial enzyme in bacterial metabolism, integral to the synthesis of cell wall components, specifically in the biosynthesis of peptidoglycan and lipopolysaccharides that constitute the structural basis of bacterial cell walls. Due to the critical role of this enzyme in maintaining bacterial cell wall integrity and viability, the inhibition of GP6 synthase has become a validated technique for the

rational design and development of innovative broad-spectrum antibacterial medicines. This enzyme-inhibition strategy presents considerable benefits compared to conventional antibiotic methods, as it focuses on a universally critical bacterial pathway, rendering it especially effective against drug-resistant bacterial strains that have acquired resistance to standard antibiotics via alternative mechanisms. The strategic targeting of GP6 synthase utilizes our comprehension of bacterial biochemistry and establishes a mechanistic basis for structure-activity relationship (SAR) studies, allowing researchers to enhance ligand binding and inhibitory efficacy through systematic molecular alterations. Thus, GP6 synthase remains a prominent target for antimicrobial drug development, and the investigation of new chemical scaffolds that can effectively inhibit this enzyme constitutes a strategic and scientifically valid method for combating the global challenge of antibiotic resistance (6, 7).

Herein, novel pyrazole and diazepine derivatives will be proposed, characterized, and biologically evaluated through molecular docking and biological assays. Major aims include finding compounds with incredible antibacterial and anticancer activity, elucidating their interaction with target proteins, and correlating their chemical structure to biological functions. The associated strategy intends to expedite the discovery of potent bioactive molecules while providing new pharmacological avenues.

2. Materials and Methods

2.1 Materials

The materials used in the study included 4-amino aniline (97% purity, Merck, Germany), 4-hydroxy aniline, 2,4-dinitrophenylhydrazine, 2,4-diaminobenzene (97% purity, Sigma Aldrich, USA), and 4-butoxy aniline (99% purity, Merck, Germany); potassium hydroxide (KOH), hydrochloric acid, and ethanol (99% purity, Merck, Germany). All chemicals were of analytical grade and were used without purification.

2.2 Methods

Synthesis of (2E)-1-(4-aminophenyl)-3-(4-substitutedphenyl) prop-2-en-1-one (1-3)

Chalcone derivatives (1-3) were synthesized from 4-aminoacetophenone and reacted with other aromatic aldehyde derivatives, including 4-aminobenzaldehyde, 4-hydroxybenzaldehyde, and 4-butoxybenzaldehyde, in the presence of potassium hydroxide (KOH) in ethanol. This mixture was refluxed for 3 h. At the end of the reflux, the reaction was subsequently acidified using 1 M hydrochloric acid to adjust the pH to pH 3. Thus, the precipitate formed is collected by filtration and washed using ethanol to afford the desired chalcone compounds (8).

Synthesis of 4-[3-(4-aminophenyl)-1-phenyl-4,5-dihydro-1H-pyrazol-5-yl]-4-substituted benzene

To prepare pyrazole derivatives (4-6), chalcone (1-3) (0.005 mol) was dissolved in ethanol, and 2,4-dinitrophenylhydrazine (1.01 g, 0.005 mol) and 0.5 mL of acetic acid were added. The above mixture was refluxed for 12 h. After completion, the reaction mixture was purified, and the product was washed with ethanol to yield the corresponding pyrazole derivatives (9).

Synthesis of 4-[4-(4-aminophenyl)-1H-1,5-benzodiazepin-2-yl]-4-substitutedbenzene

Chalcone (1-3) (0.005 mol) was dissolved in ethanol. Further, 2,4-diaminobenzene (0.99 g, 0.005 mol) and 0.5 mL of acetic acid were added. Then, the reaction is allowed to cool and refluxed. At last, filtration of the solution was done. The resulting solid was washed with ethanol to obtain diazepine derivatives (10).

2.3 Molecular Docking Studies

The three-dimensional structure of Glucosamine-6-Phosphate synthase (GP6 synthase; PDB code: 1MOQ), obtained from the Protein Data Bank, was prepared for docking through its energy minimization using Swiss-PdbViewer (version 4.1), removing water molecules and co-crystallized ligands, correcting the structure itself, and adding polar hydrogens (11). Synthesized compounds were drawn using ChemDraw Ultra (version 18.0) and energy minimized again with Chem3D (version 18.0). Conversion of all molecules into PDB format was done using Open Babel. PDBQT preparation of both enzyme and ligands was done by AutoDock Tools (version 1.5.6). Docking studies were conducted using AutoDock Vina and AutoGrid employing a gridbox (60 Å × 60 Å × 60 Å) centered on the coordinates (29.814, 21.637, -2.056). All default parameters were used, and each ligand was made to generate nine conformations. Docking results were visualized using Discovery Studio.

2.4 Antibacterial Activity Assessment

The antibacterial evaluation of synthesized derivatives (5, 6, 7, and 9) was conducted using the cup-plate agar diffusion method. The inhibition zones measured in mm were compared to the standard, which was amoxicillin in concentrations of 100, 50, and 25 µg/mL. The screened derivatives were tested on *S. aureus* (Gram-positive) and *E. coli* (Gram-negative) strains isolated from clinical samples.

Muller-Hinton agar was used as a growth medium. Sterilized agar was poured into petri dishes and allowed to solidify. Microbial suspensions were evenly spread onto the agar surface. To create wells in the agar, sterile stainless-steel cylinders (12 mm diameter) were placed on the agar, and then into these wells were added the synthesized compounds at the specified concentrations using DMSO as the solvent. Amoxicillin was dissolved in sterile distilled water. The plates were kept at an incubator temperature of 37°C for 48 hours, and the diameters of inhibition zones were recorded (12).

2.5 Cytotoxicity Evaluation Using MTT Assay

The cytotoxic effects on derivative 5 were assessed using the MTT test with a commercially available kit from Intron Biotech. In summary, 4.5×10^5 MCF-7 cells were inoculated into the wells of a 96-well plate, each containing 200 μ L of complete culture media, and incubated at 37°C for 24 hours in a 5% CO₂ environment. The incubation medium was subsequently substituted with 200 μ L of a two-fold serially diluted derivative at concentrations of 20, 40, 80, 160, and 320 μ g/mL. Each concentration was evaluated in triplicate, accompanied by suitable controls. The plates were subsequently incubated for 48 hours under identical conditions. Thereafter, 10 μ L of MTT solution was introduced to each well, and the plates were incubated for an additional 4 hours. The medium was then eliminated, and 100 μ L of DMSO solubilization solution was introduced to each well and incubated for 5 minutes. Absorbance was quantified at 575 nm utilizing an ELISA reader (Bio-Rad, Germany). The optical density readings were utilized to determine the IC₅₀ value by statistical analysis (13).

2.6 Statistical Analysis

Statistical analysis was conducted with GraphPad Prism 8 software. All experiments were conducted a minimum of three times, and the data are reported as means \pm standard deviations. One-way or two-way analysis of variance (ANOVA) using repeated measures was utilized to evaluate the significance of differences between groups. Statistical significance was established as * $p < 0.05$, ** $p < 0.01$, *** $p < 0.001$, and **** $p < 0.0001$.

3. Result

3.1 FTIR Spectroscopy Analysis

The FT-IR spectra for the synthesized compounds provided convincing and elaborate information regarding the successful transformation of chalcone derivatives (1-3; Fig. 1) into their respective pyrazole (4-6; Fig. 2) and diazepine (7-9; Fig. 3) derivatives. In the case of chalcone derivatives, FT-IR spectra exhibited strong absorption bands for aromatic C-H stretching (3042-3142 cm^{-1}), aliphatic C-H stretching (2852-2976 cm^{-1}), and a prominent carbonyl C=O stretch (1660-1673 cm^{-1}), which are characteristic of the α , β -unsaturated ketone functionality. Bands in the range of 3300-3458 cm^{-1} established the presence of primary amine groups. Such features corroborate the established literature values for chalcone derivatives and confirm the successful synthesis of the target structures.

On formation of pyrazole and diazepine derivatives via cyclization, FT-IR spectra held evidence for the disappearance of $\alpha\beta$ -unsaturated carbonyl stretch, indicating ring closure and concomitant loss of the chalcone carbonyl group. New bands assigned to C=N stretching (1624-1652 cm^{-1}) appeared in the spectra of the pyrazole and diazepine derivatives, confirming the closure of respective rings.

For example, compound 4 exhibited aromatic C-H stretches at 3097 and 3064 cm^{-1} , C=N stretching at 1624 cm^{-1} , primary amine bands at 3471 cm^{-1} and 3366 cm^{-1} , and C-H stretching of aliphatic at 2984 cm^{-1} . Compound 5 showed 3068 cm^{-1} of aromatic C-H stretching and 2877 cm^{-1} and 2921 cm^{-1} of aliphatic C-H stretches, whereas a C=N absorption can be seen at 1643 cm^{-1} . Absorption of primary amines was seen at 3472 cm^{-1} and 3368 cm^{-1} .

Compound 6 showed aromatic C-H stretching at 3043 and 3140 cm^{-1} , aliphatic C-H at 2837 cm^{-1} and 2958 cm^{-1} , and C=N stretching at 1650 cm^{-1} , along with primary amine bands at 3287 and 3370 cm^{-1} . Aromatic C-H stretches at 3042 and 3105 cm^{-1} and aliphatic C-H at 2826 cm^{-1} and 2968 cm^{-1} , C=N stretch at 1651 cm^{-1} along with primary amine bands at 3434 cm^{-1} and 3339 cm^{-1} , were recorded for Compound 7. Aromatic C-H stretches at 3011 cm^{-1} and 3140 cm^{-1} and aliphatic C-H at 2819 cm^{-1} for Compound 8, along with C=N stretch at 1628 cm^{-1} and Hydroxyl stretch at 3378 cm^{-1} . Compound 9 exhibited aromatic C-H stretches at 3084 and 3045 cm^{-1} , aliphatic C-H at 2851 and 2989 cm^{-1} , a C=N stretch at 1652 cm^{-1} , and NH₂ bands at 3339 and 3432 cm^{-1} .

3.2 NMR analysis

The ¹H NMR spectroscopic analysis of the synthesized pyrazole and diazepine derivatives yielded positive results for their successful synthesis and structural elucidation. Each compound exhibited distinct chemical shifts and splitting patterns that are consistent with their proposed structures and with established literature on similar heterocyclic systems. Pyrazole derivatives, including 4,4'-(1-phenyl-4,5-dihydro-1H-pyrazole-3,5-dial) aniline (Fig. 4a), displayed the ¹H NMR spectrum containing a singlet at δ 9.42 ppm corresponding to the amine protons, multiple between δ 6.61–7.65 ppm for aromatic protons, doublet at δ 3.22 ppm for the methylene group, and triplet at δ 4.45 ppm attributed to the H–C–N proton. The 4-[5-(4-aminophenyl)-1-phenyl-4,5-dihydro-1H-pyrazol-3-yl] phenol (Fig. 4b) spectrum shows a singlet at δ 9.45 ppm for the amine protons, δ 9.28 ppm is attributed to the phenolic hydroxyl group, multiple at δ 7.17–7.65 ppm for aromatic protons, a doublet at δ 3.83 ppm for the methylene group, and a triplet appearing at δ 4.89 ppm for the H–C–N proton. 4-[3-(4-methoxyphenyl)-1-phenyl-4,5-dihydro-1H-pyrazol-5-yl] aniline (Fig. 4c) had the ¹H NMR spectrum displaying a singlet at δ 9.25 ppm (amine), multiple δ 7.02–7.69 ppm (aromatic), doublet δ 3.84 ppm (methylene), triplet δ 5.50 ppm (H–C–N), triplet δ 0.96 ppm (methyl), multiple δ 1.44–1.78 ppm (methylene) and triplet δ 3.99 ppm (HC–O). 4,4'-(1H-1,5-benzodiazepine-2,4-diyl) dianiline (Fig. 5a), as well as the other diazepine derivatives, had a singlet at δ 9.41 ppm for the amine protons, a multiplet at δ 7.14–8.07 ppm for aromatic protons, and a signal at δ 4.41 ppm for a free NH₂ group. These features are typical of diazepine systems and correspond to previous NMR studies on related heterocycles (14).

The spectrum of the compound 4-[4-(4-aminophenyl)-1H-1,5-benzodiazepin-2-yl] phenol (Fig. 5b) showed a singlet at δ 9.68 ppm (amine), a singlet at δ 9.07 ppm

(hydroxyl), multiple at δ 7.49–8.14 ppm (aromatic), and the signals for NH₂ and other protons were observed at δ 4.75 and 5.52 ppm, respectively. Further, the NMR data for 4-[2-(4-butoxyphenyl)-1H-1,5-benzodiazepin-4-yl] aniline (Fig. 5c) would prove the existence of NH₂ groups and the aromatic and aliphatic regions expected.

3.3 Molecular Docking

Molecular docking studies were performed on the synthesized diazepine and pyrazole derivatives against glucosamine-6-phosphate synthase (GP6 synthase, PDB code: 1MOQ). The two classes of compounds showed favorable binding affinities, with docking scores of -7.8 kcal/mol for diazepine derivatives and -7 kcal/mol for pyrazole derivatives. A detailed analysis of the docking poses showed that the diazepine derivative formed two classical hydrogen bonds between its amine group and the carboxylate groups of SER303 and SER401 in the GP6 synthase binding site. These hydrogen bonds were further supplemented by van der Waals interactions and π -alkyl interaction stabilization of the ligand-protein complex (Fig. 6a-b).

For the pyrazole derivative, similar interactions were present: a hydrogen bond was noted between the amine group and ASN305, and another hydrogen bond was observed between the hydroxyl group and LYS487 (Fig. 6c-d). π -Stacked interactions, as well as van der Waals and π -alkyl interactions, contributed to the overall stability in binding.

3.4 Antibacterial Activity

The antibacterial study on the synthesized derivatives, compounds 5, 6, 7, and 9, indicated that they were notably bactericidal, exhibiting activity against both *E. coli* and *S. aureus*. During evaluation, all tested compounds showed clear inhibition, and the extent of inhibition consistently increased in proportion to the concentration levels applied (Table 1). Among all derivatives, the pyrazole derivative Compound 5 exhibited maximum activity with larger inhibition zones, demonstrating broader-spectrum antibacterial activity compared to the other tested derivatives.

3.5 Viability MTT Assay

The cytotoxicity of the compound synthesized as derivative (5) was extensively tested on the MCF-7 breast cancer cell line using the MTT assay. The results presented reflected a dose-dependent reduction in cell viability, ranging from 100.25 \pm 0.64% to 47.31 \pm 13.60%, at the highest tested dose after 24 hours, indicating that derivative (5) has significant cytotoxic effects on MCF-7 cells and that this activity increases with concentration (Fig. 7a). The calculated IC₅₀ value of derivative (5) determined in this work is 233.41 \pm 8.54 μ g/mL, which is quite high but still meaningful to cytotoxicity as compared to some of the most potent reported in the category (Fig. 7b).

Table 1. Inhibition zones (mm) of synthesized derivatives (Compounds 5, 6, 7, and 9) against *Escherichia coli* and *Staphylococcus aureus* at different concentrations (μ g/mL).

	Concentration (μ g/mL)	Compound 5	Compound 6	Compound 7	Compound 9
<i>E. coli</i>	100	33.67 \pm 3.51	29.67 \pm 2.51	27.33 \pm 1.53	25.67 \pm 2.52
	50	28.00 \pm 2.00	27.33 \pm 3.05	30.00 \pm 1.00	25.00 \pm 2.00
	25	24.67 \pm 1.53	19.67 \pm 3.51	15.67 \pm 2.52	17.33 \pm 2.08
<i>S. aureus</i>	100	19.67 \pm 1.53	7.33 \pm 1.53	15.33 \pm 2.08	9.67 \pm 2.51
	50	14.67 \pm 3.51	6.33 \pm 1.53	10.67 \pm 1.53	8.67 \pm 2.52
	25	9.67 \pm 1.53	4.33 \pm 0.58	6.67 \pm 1.53	4.67 \pm 0.58

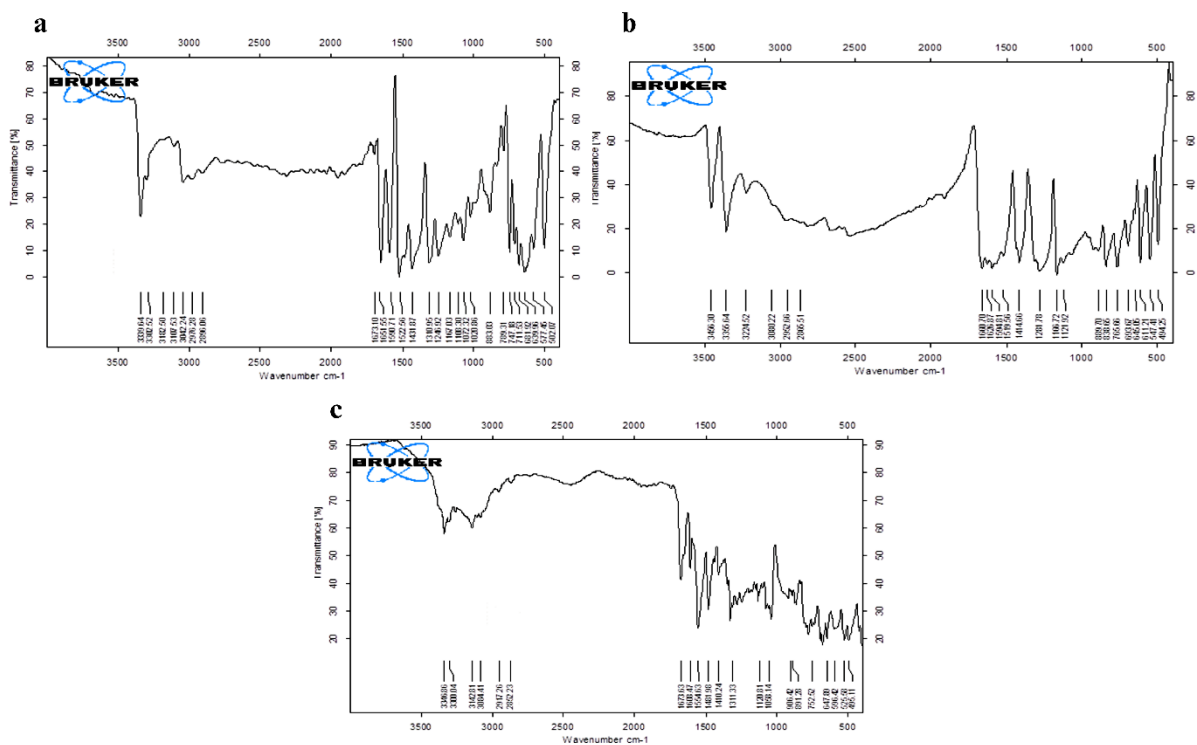


Figure 1. FT-IR spectra of synthesized compounds (a) compound 1, (b) compound 2, and (c) compound 3 (Prepared by Authors, 2025).

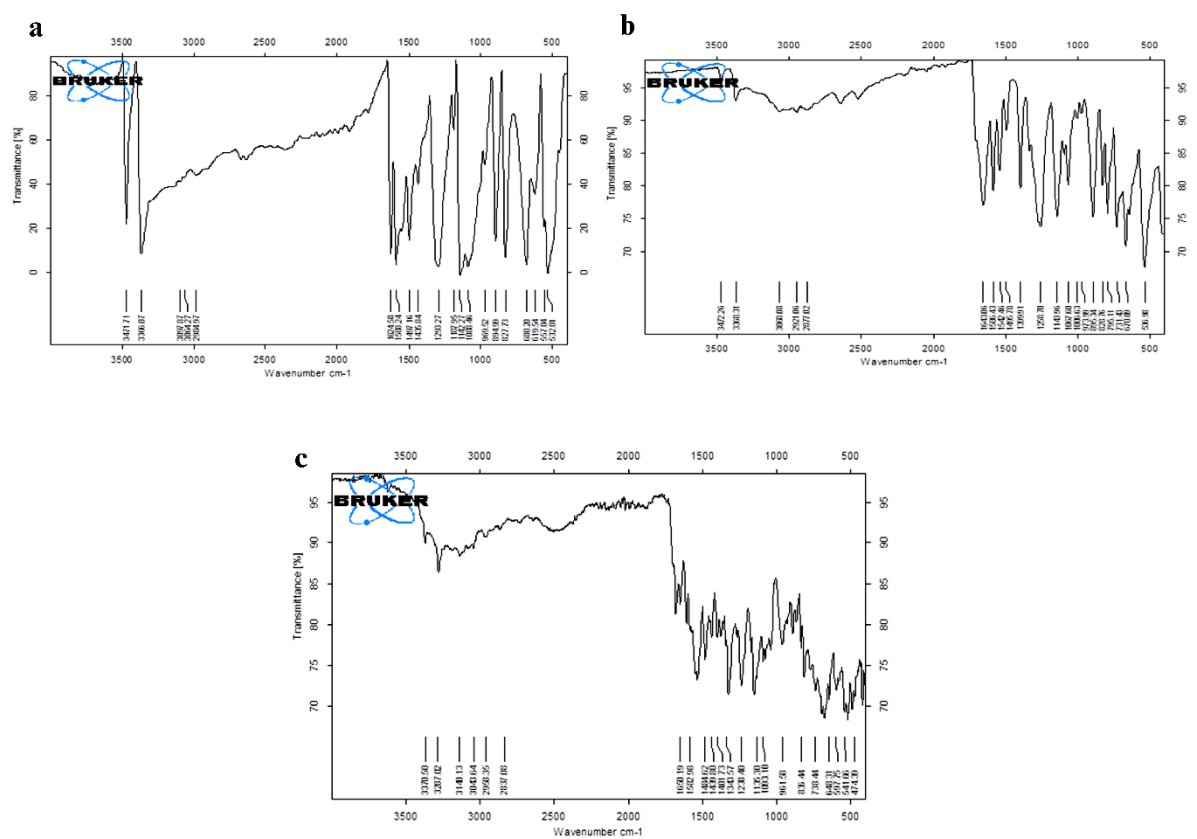


Figure 2. FT-IR spectra of synthesized compounds (a) compound 4, (b) compound 5, and (c) compound 6 (Prepared by Authors, 2025).

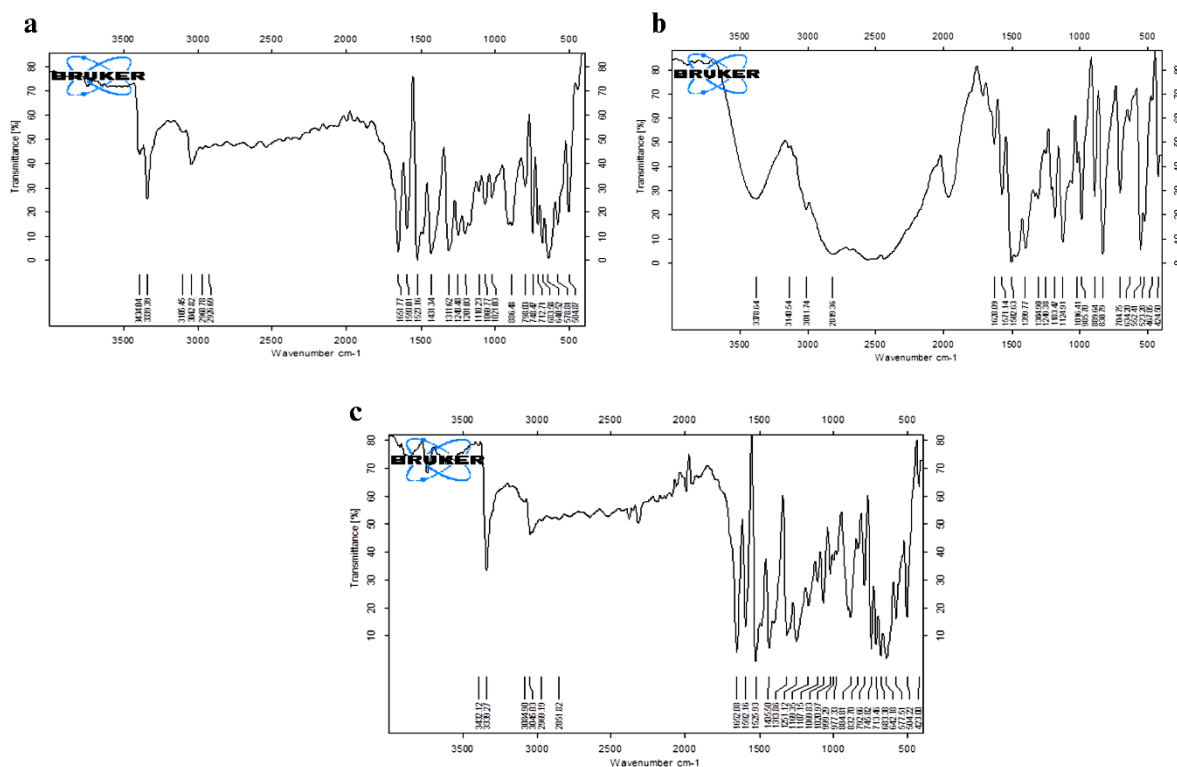


Figure 3. FT-IR spectra of synthesized compounds (a) compound 7, (b) compound 8, and (c) compound 9 (Prepared by Authors, 2025).

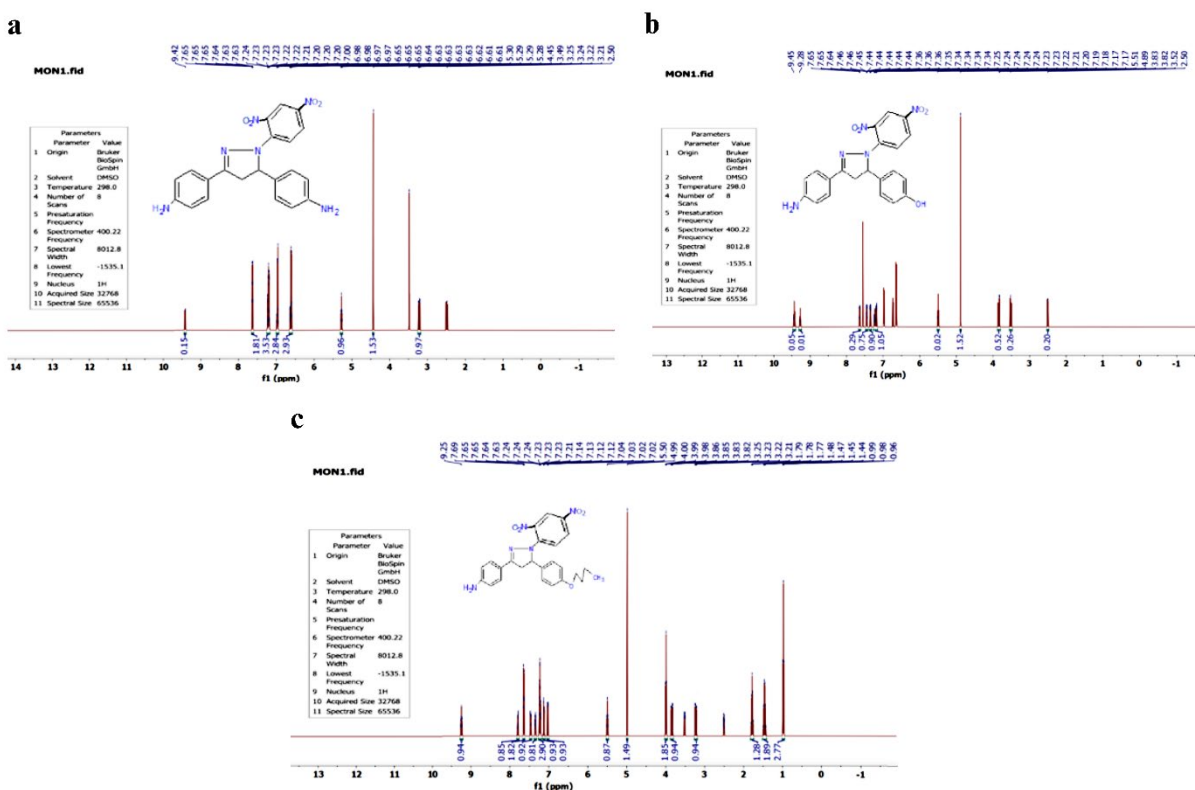


Figure 4. ^1H NMR spectra of synthesized pyrazole and diazepine derivatives: (a) 4,4'-(1-phenyl-4,5-dihydro-1H-pyrazole-3,5-diyl) aniline (4), (b) 4-[5-(4-aminophenyl)-1-phenyl-4,5-dihydro-1H-pyrazol-3-yl] phenol (5), and (c) 4-[3-(4-methoxyphenyl)-1-phenyl-4,5-dihydro-1H-pyrazol-5-yl] aniline (6), recorded in DMSO- d_6 at 400 MHz (Prepared by Authors, 2025).

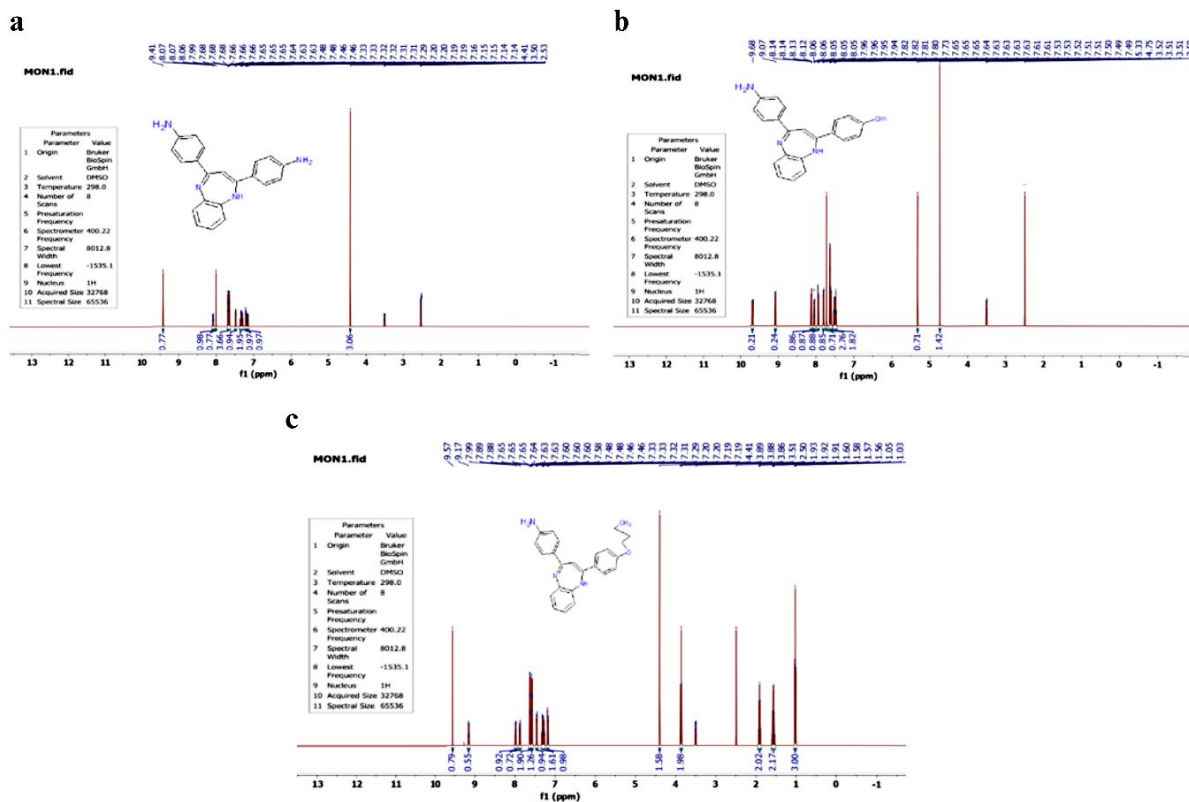


Figure 5. ¹H NMR spectra of synthesized pyrazole and diazepine derivatives: **(a)** 4,4'-(1H-1,5-benzodiazepin-2,4-diyl)dianiline (7), **(b)** 4-[4-(4-aminophenyl)-1H-1,5-benzodiazepin-2-yl]phenol (8), and **(c)** 4-[2-(4-butoxyphenyl)-1H-1,5-benzodiazepin-4-yl]aniline (9), recorded in DMSO-d₆ at 400 MHz (Prepared by Authors, 2025).

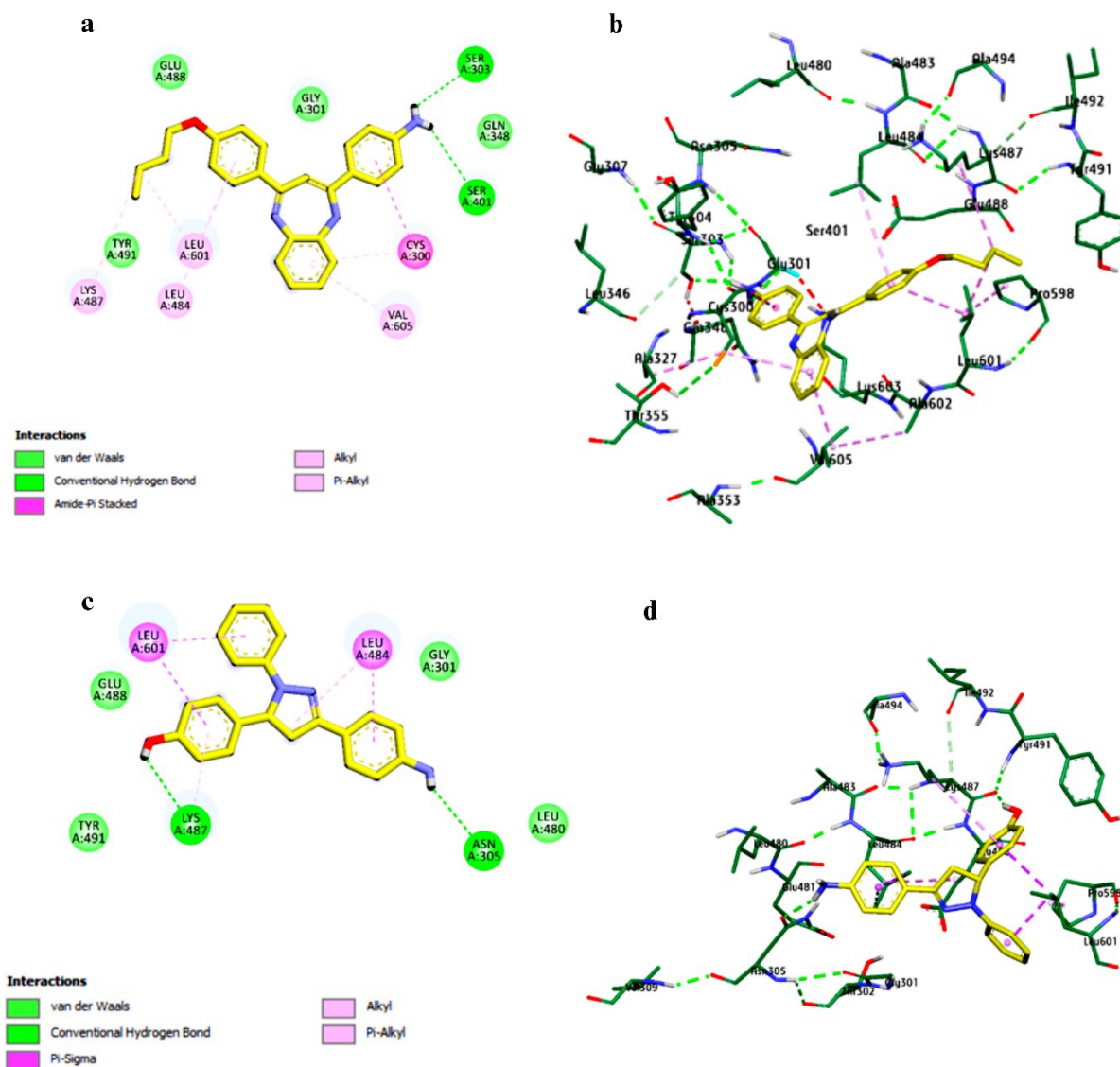


Figure 6. 2D and 3D molecular docking interaction diagrams. **(a)** 2D interaction diagram of diazepine derivative (Compound 5) with Glucosamine-6-Phosphate synthase GP6 synthase. **(b)** 3D visualization of diazepine derivative (Compound 5) docked within the active site of GP6 synthase. **(c)** 2D interaction diagram of pyrazole derivative (Compound 6) with GP6 synthase. **(d)** 3D visualization of pyrazole derivative (Compound 6) docked within the active site of GP6 synthase (Prepared by Authors, 2025).

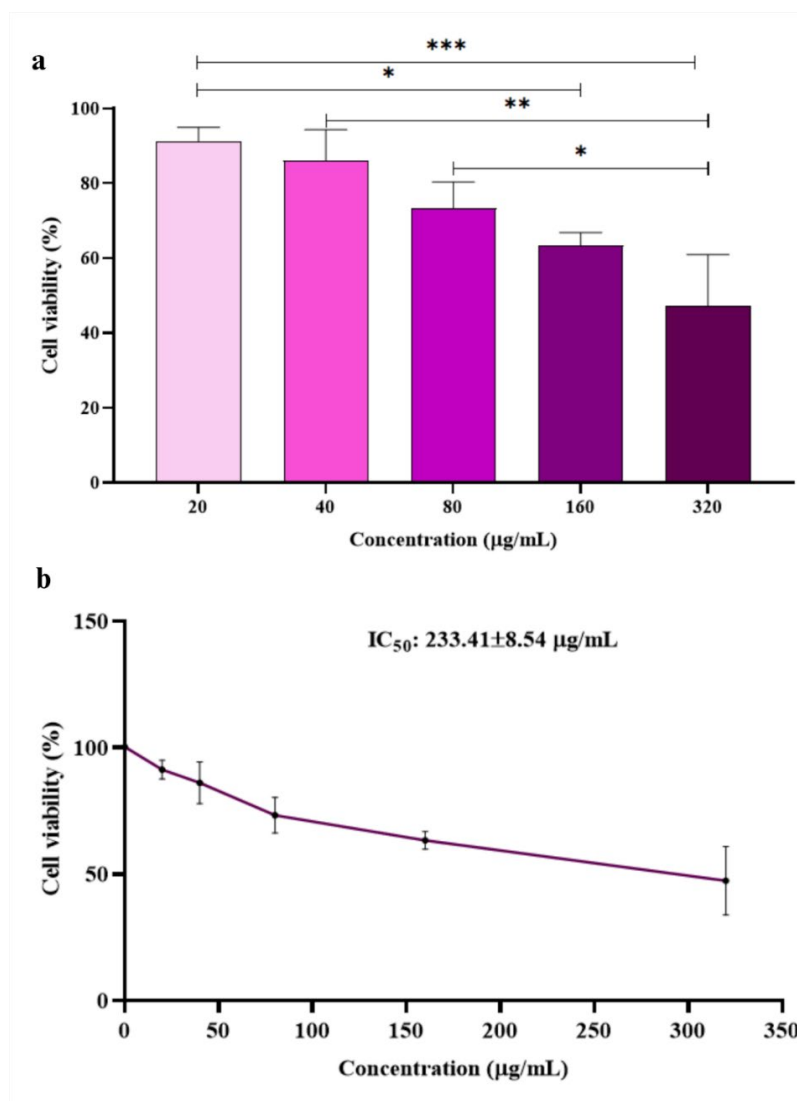


Figure 7. (a) Dose-dependent cytotoxicity of derivative (5) on MCF-7 breast cancer cells measured by MTT assay. (b) Dose-response curve illustrating decreased cell viability (%) with increasing concentrations of derivative (5), and the calculated IC_{50} value ($233.41 \pm 8.54 \mu\text{g/mL}$) (Prepared by Authors, 2025).

4. Discussions

The systematic disappearance of the carbonyl and H–C=C bands in FT-IR spectra of the cyclized products, as the C=N stretches appear, provides solid evidence for the conversion of chalcone intermediates to pyrazole and diazepine derivatives. These spectral changes correlate excellently with previous studies in similar heterocyclic syntheses in which loss of the α , β -unsaturated carbonyl and appearance of C=N bands are considered diagnostic for ring closure and heterocycle formation. Melting points, yields, and colors as physical properties further support the purity and successful isolation of synthesized compounds. Strong primary amine and the aromatic C–H stretching bands from all derivatives corroborate established spectral data for these heterocyclic systems. It is common for many research works to refer to the FT-IR chalcone spectra in a manner such that they have prominent carbonyl stretching vibrations at 1650 to 1675 cm^{-1} , which disappear upon ring closure for forming pyrazoles or diazepines with new C=N stretching

vibrations in the range of ca. 1620–1650 cm^{-1} , which in turn represent a good signature for the successful closure of cyclization and transformation (15, 16). It is generally accepted that the aromatic C–H stretching bands and the primary amine stretching bands occurring in the precursor and respective product spectra confirm faithfully the various assignments put forth in the present study (16, 17). Besides, the conversion of chalcones into pyrazole and diazepine derivatives, together with associated visible changes, has been discussed elsewhere in the literature. The disappearance of the carbonyl band with the presence of a C=N band has been mentioned time and again as strong evidence for these transformations (18, 19).

The chemical shifts and multiplicities observed for the pyrazole derivatives are in excellent agreement with established literature for similar heterocyclic systems, confirming the presence of the pyrazole ring and its substituents (20, 21). Specifically, the H–C–N proton

triplet and the methylene doublet, characteristic of the pyrazoline ring, were clearly observed. For the derivative 4-[5-(4-aminophenyl)-1-phenyl-4,5-dihydro-1H-pyrazol-3-yl] phenol, the presence of the phenolic OH group, identified by the singlet at δ 9.28 ppm, and the expected aromatic region corroborate the successful functionalization of the pyrazole core, consistent with related research. In the case of 4-[3-(4-methoxyphenyl)-1-phenyl-4,5-dihydro-1H-pyrazol-5-yl], the presence of methoxy (δ 3.99 ppm) and methyl (δ 0.96 ppm) signals further supports the expected structure, aligning well with reported NMR data for analogous compounds. The spectral features of the diazepine derivatives, including the singlet for the amine protons and the multiple for aromatic protons, are typical of diazepine systems and correspond to previous NMR studies on related heterocycles (21). The clear identification of both the amine and hydroxyl protons for 4-[4-(4-aminophenyl)-1H-1,5-benzodiazepin-2-yl] phenol further confirms the structure under discussion. The observation of NH₂ groups and the expected aromatic and aliphatic regions in 4-[2-(4-butoxyphenyl)-1H-1,5-benzodiazepin-4-yl] aniline NMR data further validates its structure based on available literature. These findings, substantiated by previous research, strongly confirm that ¹H NMR spectroscopy provides strong arguments in the structural elucidation of pyrazole and diazepine derivatives (22). The consistency of the chemical shifts, multiplicities, and integration values observed confirms the successful synthesis and correct structural assignment of the new derivatives (23). ¹H NMR, combined with other spectroscopic methodologies, is well recognized as standard practice for the characterization of heterocyclic compounds (24).

The favorable binding affinities observed for both compound classes, indicated by the strong docking scores, suggest a strong and stable interaction within the active site of the enzyme, positioning these molecules as prospective inhibitors. The GP6 synthase binding mechanism observed for the diazepine derivative, characterized by a combination of hydrogen bonding (with SER303 and SER401) and hydrophobic interactions (π -alkyl and van der Waals), is well recognized in the literature to be crucial for achieving high-affinity binding and effective inhibition of target enzymes (25, 26). Similarly, the binding profile of the pyrazole derivative, which involved a hydrogen bond between the amine group and ASN305 and another between the hydroxyl group and LYS487, is consistent with prior studies. These studies demonstrate that the binding mechanisms of pyrazole-based ligands typically involve a combination of hydrogen bonds and hydrophobic interactions with key amino acid residues in the target protein (27, 28). Similar binding affinities and interaction outlines have been reported in other literature studies of heterocyclic compounds, with comparable docking scores for bioactive pyrazole and diazepine derivatives targeting various enzymes and receptors (29). The specific hydrogen bond interactions highlighted herein, particularly with SER303, SER401, ASN305, and

LYS487, suggest that the functional group orientation and electronic properties are crucial for enhancing ligand-protein binding, a principle supported by earlier computational and experimental studies (26).

The pronounced efficacy demonstrated by derivative 5 is likely due to its structural peculiarities, particularly the presence of diamino and dinitro functional groups. These substituents facilitate the crucial interaction of the heterocyclic backbone with bacterial targets, thereby enhancing otherwise modest properties. This observation is corroborated by findings from earlier research where pyrazole derivatives bearing electron-donating or electron-withdrawing substituents, such as amino and nitro groups, were reported to show improved antibacterial activities against both Gram-positive and Gram-negative bacteria (30, 31). Recent works have further shown that substitutions of this type in pyrazole-based compounds can yield minimum inhibitory concentration (MIC) values comparable to or even below some standard antibiotics, affirming their therapeutic prospects (32). The concentration-dependent increase in antibacterial activities observed across all tested compounds is consistent with established structure-activity relationship (SAR) patterns of pyrazole- and diazepine-type derivatives. The ability of such compounds to interfere with bacterial cell processes is typically correlated with the nature and position of the substituents around the aromatic ring, which modulate lipophilicity and electronic attributes, thus affecting membrane permeation and target binding (33).

The dose-dependent reduction in cell viability indicates that derivative (5) has significant cytotoxic effects on MCF-7 cells and that this activity increases with concentration. Such dose-response relationships are characteristic of effective anticancer agents, thereby corroborating the promising therapeutic use of this compound. The cytotoxic effect of derivative (5) is further supported by recent findings from studies on structurally related pyrazole and diazepine derivatives known to be active against a broad spectrum of human cancers, including MCF-7. For instance, several recently patented pyrazole-based compounds had IC₅₀ values in the low micromolar range against MCF-7 cells, confirming the strong antiproliferative effects of the compounds (34, 35). This also highlights the importance of specific functional groups and molecular frameworks in improving cytotoxicity, supporting the rationale for the design and selection of derivative (5) in this study. It should be noted that while the IC₅₀ value of derivative (5) is 233.41 \pm 8.54 μ g/mL, which is quite high, it is still meaningful to cytotoxicity when compared to some of the most potent reported in the category. The cytotoxic activity of pyrazole and diazepine derivatives can vary widely with structural modification, depending on substituent groups and the effect upon the target cell line into which the active derivative is being tested (36).

Furthermore, the good molecular docking profile of derivative (5) was a factor in its further investigation. This docking profile relates it to an inhibitory interaction with

the human androgen receptor (PDB ID: 1E3G), where it is assumed that a dual mechanistic approach could enhance its anticancer potential.

5. Conclusion

This research effectively produced and characterized new pyrazole and diazepine compounds by traditional organic synthesis techniques. Structural validation was accomplished via FT-IR and ¹H NMR spectroscopy, demonstrating the transformation from chalcone precursors to the target heterocyclic molecules. Crucial evidence comprised the absence of α , β -unsaturation stretching vibrations and the emergence of C=N stretching bands. Molecular docking experiments indicated that these compounds demonstrated strong binding affinities for glucosamine-6-phosphate synthase, implying their potential as enzyme inhibitors. Biological tests revealed that multiple derivatives, especially compound 5, exhibited substantial antibacterial efficacy against *E. coli* and *S. aureus*, with potency escalating in a concentration-dependent fashion. Moreover, compound 5 demonstrated significant cytotoxicity against the MCF-7 breast cancer cell line, suggesting its potential as an anticancer drug. This research is original due to its comprehensive strategy that encompasses synthesis, characterisation, molecular docking, and biological evaluation. This study emphasizes the promise of pyrazole and diazepine frameworks as viable candidates for new antibacterial and anticancer medicines, with further research aimed at compound optimization and mechanistic investigations to further examine their therapeutic uses.

6. Declarations

6.1 Acknowledgments

None.

6.2 Ethical Considerations

This study did not involve human participants or experimental animals. All experiments were conducted using established laboratory cell lines and standard bacterial strains. Therefore, ethical approval was not required.

6.3 Authors' Contributions

D. Saleem: Methodology, Software; Z. H. Ali, and N. W. Ibrahim: Visualization, Investigation; A. K. Abbas: data curation, writing—original draft preparation; T. M. Abd-Almonaem: Methodology; M. H. Al-Musawi: Methodology; M. Gharbavi: Conceptualization, writing—reviewing and editing.

6.4 Conflict of Interest

The authors declare no conflicts of interest.

6.5 Fund or Financial Support

This research received no specific grant from any funding agency in the public, commercial, or not-for-profit sectors.

6.6 Using Artificial Intelligence Tools (AI Tools)

The authors were not utilized AI Tools.

References

- Asif M, Almeahmadi M, Alsaiari AA, Allahyani M. Diverse pharmacological potential of different substituted pyrazole derivatives. *Current Organic Synthesis*. 2024;21(7):858-88. [DOI:10.2174/0115701794260444230925095804] [PMID]
- Qadir T, Amin A, Sharma PK, Jeelani I, Abe H. A review on medicinally important heterocyclic compounds. *Open Med Chem J*. 2022;16(1). [DOI:10.2174/18741045-v16-e2202280]
- Bhattacharya S, Chakraborty S, Pal R, Saha S, Ghosh B, Mandal C, et al. A Comprehensive Review on Pyrazole and Its Pharmacological Properties. *Int J Res in Appl Sci Eng Technol*. 2022;10(IX):1769-74.
- Sánchez-Céspedes J, Martínez-Aguado P, Vega-Holm M, Serna-Gallego A, Candela JI, Marrugal-Lorenzo JA, et al. New 4-acyl-1-phenylaminocarbonyl-2-phenylpiperazine derivatives as potential inhibitors of adenovirus infection. Synthesis, biological evaluation, and structure-activity relationships. *J Med Chem*. 2016;59(11):5432-48. [PMID] [DOI:10.1021/acs.jmedchem.6b00300]
- Chen H, Ma YB, Huang XY, Geng CA, Zhao Y, Wang LJ, et al. Synthesis, structure-activity relationships and biological evaluation of dehydroandrographolide and andrographolide derivatives as novel anti-hepatitis B virus agents. *Bioorg Med Chem Lett*. 2014;24(10):2353-9. [DOI:10.1016/j.bmcl.2014.03.060] [PMID]
- Walter A, Mayer C. Peptidoglycan structure, biosynthesis, and dynamics during bacterial growth. In: *Extracellular sugar-based biopolymers matrices*. 2019. pp. 237-299. Cham, Switzerland: Springer International

- Publishing. [[DOI:10.1007/978-3-030-12919-4_6](https://doi.org/10.1007/978-3-030-12919-4_6)]
- Gupta R, Gupta N, Bindal S. Bacterial cell wall biosynthesis and inhibitors. In *Fundamentals of Bacterial Physiology and Metabolism*. 2021. pp. 81-98. Singapore, Singapore: Springer Singapore. [[DOI:10.1007/978-981-16-0723-3_3](https://doi.org/10.1007/978-981-16-0723-3_3)]
 - Santiago R, Freire P, Teixeira A, Bandeira P, Santos H, Lemos TL, et al. FT-Raman and FT-IR spectra and DFT calculations of chalcone (2E)-1-(4-aminophenyl)-3-phenyl-prop-2-en-1-one. *Vib Spectrosc*. 2018;97:1-7. [[DOI:10.1016/j.vibspec.2018.04.007](https://doi.org/10.1016/j.vibspec.2018.04.007)]
 - Cai HX, Wu WN, Li XX, Wang Y. 3-Methyl-4-[[3-{{[(3-methyl-5-oxo-1-phenyl-4, 5-dihydro-1H-pyrazol-4-ylidene)(phenyl)methyl] aminomethyl} benzyl] amino}(phenyl)methylidene}-1-phenyl-1H-pyrazol-5 (4H)-one. *Struct Rep*. 2011;67(8):o2015. [[PMCID](https://pubmed.ncbi.nlm.nih.gov/26766679/)] [[DOI:10.1107/S1600536811027000](https://doi.org/10.1107/S1600536811027000)] [[PMID](https://pubmed.ncbi.nlm.nih.gov/26766679/)]
 - Loughzail M, Fernandes JA, Baouid A, Essaber M, Cavaleiro JA, Almeida Paz FA. 4-Phenyl-1-(prop-2-yn-1-yl)-1H-1, 5-benzodiazepin-2 (3H)-one. *Struct Rep*. 2011;67(8):o2075-o6. [[DOI:10.1107/S1600536811027371](https://doi.org/10.1107/S1600536811027371)] [[PMID](https://pubmed.ncbi.nlm.nih.gov/26766679/)] [[PMCID](https://pubmed.ncbi.nlm.nih.gov/26766679/)]
 - Gharbavi M, Danafar H, Amani J, Sharafi A. Immuno-informatics analysis and expression of a novel multi-domain antigen as a vaccine candidate against glioblastoma. *Int Immunopharmacol*. 2021;91:107265. [[DOI:10.1016/j.intimp.2020.107265](https://doi.org/10.1016/j.intimp.2020.107265)] [[PMID](https://pubmed.ncbi.nlm.nih.gov/34114985/)]
 - Malekzadeh H, Hussein S, Khudhair I, Nabeel A, Gharbavi M. The in vitro Study of the Synergistic Antibacterial Effect of Hydroalcoholic Mentha Extract with Alum on the Growth of *Streptococcus mutans*. *Jundishapur J Nat Pharm Prod*. 2024;19(4):e148545 [[DOI:10.5812/jjnpp-148545](https://doi.org/10.5812/jjnpp-148545)]
 - Gharbavi M, Sharafi A, Motamed Fath P, Oruji S, Pakzad H, Kheiri Manjili H. Formulation and biocompatibility of microemulsion-based PMBN as an efficient system for paclitaxel delivery. *J Appl Biotechnol Rep*. 2021;8(1):e114985.
 - Tutar Y. Diazepine Derivative Compounds as Heat Shock Protein 90 Inhibitor in Oncology. *Drug Des*. 2015;4:e127. [[DOI:10.4172/2169-0138.1000e127](https://doi.org/10.4172/2169-0138.1000e127)]
 - E. Hawaiz F, K. Samad M. Synthesis and spectroscopic characterization of some new biological active azo-pyrazoline derivatives. *J Chem*. 2012;9(3):1613-22. [[DOI:10.1155/2012/525940](https://doi.org/10.1155/2012/525940)]
 - Jagadhani S, Kundlikar S, Karale B. Synthesis and characterization of some fluorinated 1, 5-benzothiazepines and pyrazolines. *Orient J Chem*. 2015;31:601-4. [[DOI:10.13005/ojc/310177](https://doi.org/10.13005/ojc/310177)]
 - Yaseen LA, Al-Amood HK. Preparation, Characterization, and Study of Antibacterial some new Pyrazole Derivatives. *J Kufa Chem Sci*. 2022;2(9):304-18. [[DOI:10.36329/jkcm/2022/v2.i9.13304](https://doi.org/10.36329/jkcm/2022/v2.i9.13304)]
 - Rana M, Hungyo H, Parashar P, Ahmad S, Mehendi R, Tandon V, et al. Design, synthesis, X-ray crystal structures, anticancer, DNA binding, and molecular modelling studies of pyrazole-pyrazoline hybrid derivatives. *RSC Adv*. 2023;13(38):26766-79. [[PMID](https://pubmed.ncbi.nlm.nih.gov/41811111/)] [[PMCID](https://pubmed.ncbi.nlm.nih.gov/41811111/)] [[DOI:10.1039/D3RA04873J](https://doi.org/10.1039/D3RA04873J)]
 - Shehab WS, Elhoseni NKR, Aboulthana WM, Assy MG, Mousa SM, El-Bassyouni GT. Synthesis, molecular docking, assessment of biological and anti-diabetic properties of benzalacetophenone derivatives. *Sci Rep*. 2025;15(1):14159. [[PMID](https://pubmed.ncbi.nlm.nih.gov/45811111/)] [[PMCID](https://pubmed.ncbi.nlm.nih.gov/45811111/)] [[DOI:10.1038/s41598-025-96610-6](https://doi.org/10.1038/s41598-025-96610-6)]
 - Mustafa G, Sabir S, Sumrra SH, Zafar W, Arshad MN, Hassan AU, et al. Synthesis, structure elucidation, SC-XRD/DFT, molecular modelling simulations and DNA binding studies of 3, 5-diphenyl-4, 5-dihydro-1 H-pyrazole chalcones. *Biomol Struct Dyn*. 2025; 43(4):1831-46. [[PMID](https://pubmed.ncbi.nlm.nih.gov/45811111/)] [[DOI:10.1080/07391102.2023.2293260](https://doi.org/10.1080/07391102.2023.2293260)]
 - Sapkota KR. Synthesis, Characterization, and Structural Elucidation of a Novel (E)-1-(1-Phenyl-1H-pyrazol-4-yl)-N-(1-(p-tolyl)-1H-pyrazol-5-yl) methanimine. *Intell Multidiscip Res*. 2025;4(1):67-80. [[DOI:10.3126/ijmr.v4i1.76932](https://doi.org/10.3126/ijmr.v4i1.76932)]
 - Bouhfid R, Lazar S, Essassi EM, Leger J-M, Jarry C, Guillaumet G. Crystal structure of (Z)-1, 3-diallyl-4-(2-oxopropylidene)-4, 5-dihydro-1H-1, 5-benzodiazepin-2 (3H)-one, C18H20N2O2. *Z fur Krist New Cryst Struct*. 2008;223(4):435-6. [[DOI:10.1524/ncrs.2008.0190](https://doi.org/10.1524/ncrs.2008.0190)]
 - Spirlet M-R, Mohsine A, Christians L. Crystal structure of N-benzyl-dibenzo [d, f]-1, 2-thiazepin-3-one, C20H15NOS. *Z fur Krist New Cryst Struct*. 1999;214(1):139-40. [[DOI:10.1515/ncrs-1999-0170](https://doi.org/10.1515/ncrs-1999-0170)]
 - Ayyash A, Juwair K, Najeeb O, Jasim N. Synthesis of New Bioactive Compounds of Pyrazino [2, 3-e][1, 3] Oxazepines and Pyrazino [2, 3-e][1, 3] Diazepines Bearing 1, 3, 4-Oxadiazole Moieties. *Egypt J Chem*. 2021; 64(6):2945-52. [[DOI:10.21608/ejchem.2021.55735.3174](https://doi.org/10.21608/ejchem.2021.55735.3174)]

25. Siliveri S, Bashaboina N, Vamaraju HB, Raj S. Design, synthesis, molecular docking, ADMET studies and biological evaluation of pyrazoline incorporated 1, 2, 3-triazole benzene sulphonamides. *Int J Pharm Pharm Sci.* 2019; 11:6-15. [DOI:10.22159/ijpps.2019v11i6.32684]
26. Salih RHH, Hasan AH, Hussein AJ, Samad MK, Shakya S, Jamalis J, et al. One-pot synthesis, molecular docking, ADMET, and DFT studies of novel pyrazolines as promising SARS-CoV-2 main protease inhibitors. *Res Chem Intermed.* 2022;48(11):4729-51. [DOI:10.1007/s11164-022-04831-5] [PMCID]
27. Belal A, Abdel Gawad NM, Mehany AB, Abourehab MA, Elkady H, Al-Karmalawy AA, et al. Design, synthesis and molecular docking of new fused 1 H-pyrroles, pyrrolo [3, 2-d] pyrimidines and pyrrolo [3, 2-e][1, 4] diazepine derivatives as potent EGFR/CDK2 inhibitors. *J Enzyme Inhib Med Chem.* 2022;37(1):1884-902. [DOI:10.1080/14756366.2022.2096019] [PMID] [PMCID]
28. Javaregowda VG, Doreswamy BH, Ningaiah S, Bhadraiah UK, Kemparaju K, Madegowda M. Molecular docking of 1H-pyrazole derivatives to receptor tyrosine kinase and protein kinase for screening potential inhibitors. *Bioinformation.* 2014;10(7):413. [PMCID] [DOI:10.6026/97320630010413] [PMID]
29. Sayed AR, Gomha SM, Abdelrazek FM, Farghaly MS, Hassan SA, Metz P. Design, efficient synthesis and molecular docking of some novel thiazolyl-pyrazole derivatives as anticancer agents. *BMC Chem.* 2019;13(1): 116. [DOI:10.1186/s13065-019-0632-5] [PMID] [PMCID]
30. Radini IAM. Design, synthesis, and antimicrobial evaluation of novel pyrazoles and pyrazolyl 1, 3, 4-thiadiazine derivatives. *Molecules.* 2018;23(9):2092. [PMCID] [DOI:10.3390/molecules23092092] [PMID]
31. A Alam M. Antibacterial pyrazoles: Tackling resistant bacteria. *Future Med Chem.* 2022; 14(5):343-62. [DOI:10.4155/fmc-2021-0275] [PMID] [PMCID]
32. Burke A, Di Filippo M, Spiccio S, Schito AM, Caviglia D, Brullo C, et al. Antimicrobial evaluation of new pyrazoles, indazoles and pyrazolines prepared in continuous flow mode. *Int J Mol Sci.* 2023;24(6):5319. [PMCID] [DOI:10.3390/ijms24065319] [PMID]
33. Marinescu M. Synthesis of antimicrobial benzimidazole-pyrazole compounds and their biological activities. *Antibiotics.* 2021;10(8): 1002. [DOI:10.3390/antibiotics10081002] [PMID] [PMCID]
34. Shawky AM, Ibrahim NA, Abourehab MA, Abdalla AN, Gouda AM. Pharmacophore-based virtual screening, synthesis, biological evaluation, and molecular docking study of novel pyrrolizines bearing urea/thiourea moieties with potential cytotoxicity and CDK inhibitory activities. *J Enzyme Inhib Med Chem.* 2021;36(1):15-33. [PMID] [PMCID] [DOI:10.1080/14756366.2021.1937618]
35. Alaa AM, El-Azab AS, Brogi S, Ayyad RR, Alkahtani HM, Abuelizz HA, et al. Synthesis, enzyme inhibition assay, and molecular modeling study of novel pyrazolines linked to 4-methylsulfonylphenyl scaffold: antitumor activity and cell cycle analysis. *RSC Adv.* 2024;14(31):22132-46. [PMID] [PMCID] [DOI:10.1039/D4RA03902E]
36. Zhang Y, Wu C, Zhang N, Fan R, Ye Y, Xu J. Recent advances in the development of pyrazole derivatives as anticancer agents. *Int J Mol Sci.* 2023;24(16):12724. [PMCID] [DOI:10.3390/ijms241612724] [PMID]

How to Cite This Article:

Saleem D, Ali ZH, Ibrahim NW, Abbas AK, Abd-Almonaem TM, Al-Musawi MH, et al. Exploring Pyrazole and Diazepine Derivatives: Advances in Molecular Docking, Synthesis, and Biological Activities. *J Adv Med Biomed Res.* 2025;33(161):358-71.

Download citation:

[BibTeX](#) | [RIS](#) | [EndNote](#) | [Medlars](#) | [ProCite](#) | [Reference Manager](#) | [RefWorks](#)

Send citation to:

 [Mendeley](#)  [Zotero](#)  [RefWorks](#)